Hot-electron mean free path of ErAs thin films grown on GaAs determined by metal-base transistor ballistic electron emission spectroscopy

K. J. Russell* and V. Narayanamurti
Gordon McKay Laboratory, Harvard University, Cambridge, Massachusetts 02138, USA

Ian Appelbaum
Electrical and Computer Engineering Department, University of Delaware, Newark, Delaware 19716, USA

M. P. Hanson and A. C. Gossard
Materials Department, University of California, Santa Barbara, California 93106, USA
(Received 21 July 2006; revised manuscript received 15 September 2006; published 22 November 2006)

We present an experimental investigation of the hot-electron mean free path in ErAs thin films grown on GaAs. Using an $Al/Al_2O_3/Al$ tunnel junction as a hot-electron source for ballistic electron emission spectroscopy, we investigate ErAs films of thicknesses $\sim 100-\sim 300$ Å. Our results indicate a mean free path of order 100 Å for electrons 1–2 eV above the Fermi level at 80 K.

DOI: 10.1103/PhysRevB.74.205330 PACS number(s): 73.61.−r, 72.15.Lh, 72.80.Jc, 73.23.Ad

ErAs is a semimetal[1] that can be grown epitaxially on GaAs[1,2] and InGaAs/InAlAs lattice-matched to InP.[2,3] Recently the ErAs/InAlGaAs system has been used to demonstrate tunable Schottky barrier heights,[4] high sensitivity microwave detectors,[5] and low-noise Schottky diodes.[6] Although epitaxial overgrowth on continuous ErAs films has proven difficult,[1] isolated ErAs nanoparticles can be grown throughout the host matrix without degrading the crystal quality.[2,3] This technique has been used to create subpicosecond photomixers in both GaAs (Refs. 7–9) and InGaAs,[10] as well as to increase the efficiency of thermal energy converting devices[11,12] and multijunction solar cells.[13] Yet despite the promising characteristics of ErAs and its compatibility with GaAs and InGaAs, there has been relatively little experimental investigation of its basic physical properties.[1,7,14] It is in this vein that we present the following investigation of the hot-electron mean free path in ErAs thin films grown on GaAs. This parameter should prove useful for design and optimization of ErAs devices for ultrafast or high-temperature applications.

Using a solid-state tunnel junction as a hot electron source, we perform a spatially averaged version of electron spectroscopy based on ballistic electron emission microscopy/spectroscopy.[15–18] In these devices, an $Al/Al_2O_3/Al$ tunnel junction injects electrons into a metallic base, which they must traverse to enter a semiconductor collector [Fig. 1(a)]. The probability of entering the collector depends on the energy of the electron, which is varied by changing the tunnel junction bias. By dividing the collector-base current I_{CB} by the emitter-base current I_{EB}, we arrive at the transfer ratio, an energy-dependent characterization of hot-electron transport through the device.

In a single device we can use the energy-dependent transfer ratio to investigate characteristics such as momentum conservation at the base-collector interface.[14] This same measurement can be made on multiple devices with different base layer thicknesses, and comparisons between the transfer ratios of the individual devices can be used to find the energy-dependent mean free path of the base layer.[17]

The semiconductor collector for all samples studied in this work is of the same structure: 100 nm GaAs *n*-type doped to 1×10^{17} cm^{-3} grown via MBE on (100) *n*-GaAs substrates. The base of the transistor is grown on the collector *in situ* and is comprised of a film of ErAs of thickness d_{ErAs} capped with ~100 Å Al. This Al overlayer protects the ErAs from oxidation, but because it also reacts with oxygen in the air, we are unable to use a scanningtunneling microscopy (STM) tip for electron injection.[17] Instead, we use a device geometry with the native Al oxide as the tunnel barrier for electron emission.

Four samples were grown with varying ErAs film thickness. This was done on two separate growth runs, one for samples with $d_{ErAs}=120$ and 180 Å and another run with $d_{ErAs}=138$ and 276 Å. These values are ±5 Å, as measured by x-ray diffraction. It is significant that the samples were grown during different growth runs becasuse the *in situ* evaporation rate of Al was estimated by the Al flux. Since our analysis requires identical Al layer thicknesses to make an accurate estimate of ErAs mean free path (as explained below), the lack of accurate Al thickness monitoring during deposition prevents us from being able to make cross comparisons between samples grown during different runs.

After collector and base fabrication, the sample was removed from the MBE system for further processing, which has been described elsewhere.[14] See Fig. 1(b) for an optical image of the final device.

All measurements were performed in common-base configuration at 80 K. These consisted of monitoring both I_{EB} and I_{CB} while varying the emitter voltage V_{EB} at zero collector bias. See trace "a" of Fig. 2 for an example of the dependence of I_{CB} on V_{EB} for values of eV_{EB} near the Schottky barrier [~0.85 eV. (Ref. 14)]

While there are obvious advantages of being able to deposit the base layer *in situ*, there are also a few drawbacks. Upon removing the sample from the MBE system, the emitter structure is deposited as soon as possible to achieve tunnel junctions that are conductive enough to be useful. This prevents us from etching the base layer into devices prior to

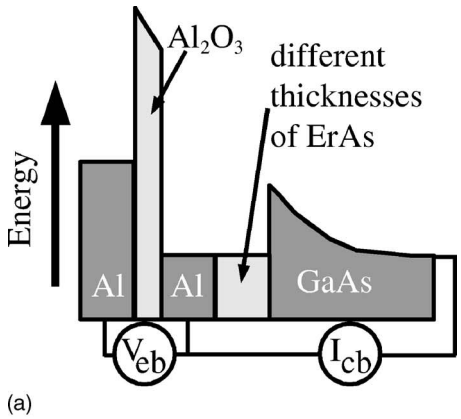

(a)

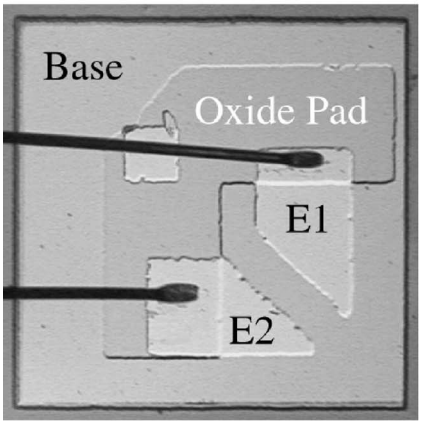

(b)

FIG. 1. (a) Schematic conduction band diagram for an Al/ErAs metal-base transistor with nonzero emitter bias. Electrons tunnel across the Al_2O_3 barrier and enter the Al/ErAs base region at an energy approximately equalto eV_{EB}. For sufficient eV_{EB}, a fraction of electrons will traverse the base region and overcome the Schottky barrier to enter the GaAs collector. (b) Image of a working device. The Al/ErAs base is continuous across the mesa, and bonding wires contact each emitter ($E1$ and $E2$) above the Al_2O_3 bonding pad. One emitter is shorted to form an Ohmic contact to the Al/ErAs base.

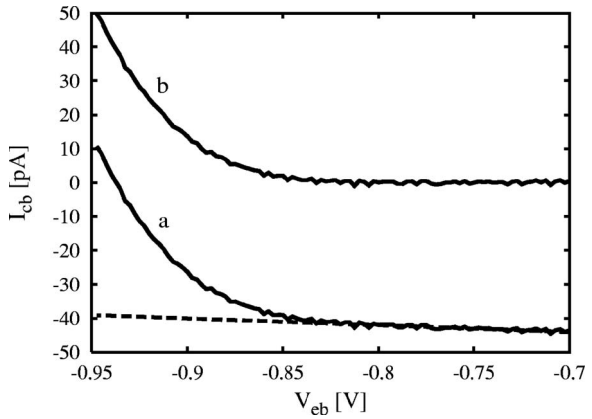

FIG. 2. Representative trace of collector current I_{CB} versus emitter bias V_{EB} from a 120 Å ErAs device for a range of V_{EB} near the onset of I_{CB}. The real data (trace "a") shows ~−40 pA electrometeroffset as well as linear parasitic leakage at lower values of $|V_{EB}|$. This leakage is fitted with a line (dashed), which is then subtracted from the real data to arrive at the data used for analysis (trace "b"). This corrected data is divided by the emitter current I_{EB} to yield the transfer ratio.

emitter deposition, and, as a result, the base layer of the device extends underneath the bonding pad [see Fig. 1(b)]. The Schottky barriers of our devices have larger reverse-bias currents than expected for a 0.85 eV Schottky barrier at 80 K (typically a few 100 pA at 1 V), which we suspect is due to to either degradation of the ErAs/GaAs interface in the region below the bond or surface leakage from residual Er left after base layer etching. This problem is compounded by the fact that the contact to the base layer is formed by shorting through the native Al_2O_3. This process is difficult to control and the resulting contact to the base layer is still slightly resistive. By comparing the subthreshold leakage of I_{CB} (the dashed trace in Fig. 2) with the reverse-bias leakage of the Schottky barrier, we estimate a typical base-contact resistance of 1 kΩ. This resistance forms a voltage divider with the emitter tunnel junction (which is ~10 kΩ at biases near E_{SB}/e), effectively reverse-biasing the collector Schottky barrier by a fraction of V_{EB} and leading to the observed subthreshold leakage. It should be noted this base-contact resistance also leads to a slight overestimate of E_{SB} because the electron energy relative to the Fermi level of the base metal will be lower than eV_{EB} by an amount equal to the voltage dropacross the base-contact resistance. In light of this correction, our measurement of $E_{SB} \sim 0.85$ eV (Ref. 14) could be conservatively viewed as an upper bound, with the real value lying closer to $E_{SB} \sim 0.80$ eV.

To enable the analysis that follows, we fit the subthreshold dependence of I_{CB} (trace "a" in Fig. 2) with a line (the dashed trace in Fig. 2). We then subtracted the fitted line from the original data to yield a trace that was corrected for the Schottky leakage as well as electrometer offset (trace "b" in Fig. 2). This subtraction relies on two assumptions, both of which are accurate enough for the order-of-magnitude analysis we aim to achieve in this paper. The first assumption is that the reverse leakage of the Schottky barrier is linear for small collector-base biases (≤200 mV). This is true to within the noise of our system (few pA). Secondly, by subtracting a line from the data for all values of V_{EB}, we are assuming that the tunnel junction has a linear current-voltage relationship, which is not the case. However, this is not a serious concern because the values that we are subtracting are only tens of pA even at the highest emitter energies, whereas I_{CB} quickly increases to values much larger than this for $V_{EB} > E_{SB}$. As a result, our analysis is more accurate for higher electron energies.

We begin our analysis with a simple integral expression for I_{CB}:

$$I_{CB}(V) = \int_0^{eV_{EB}} P(E, V_{EB}) e^{-d/\lambda(E)} SC(E) dE, \qquad (1)$$

where V_{EB} is emitter-base voltage, E is electron energy above the Fermi level in the base, λ is the mean free path for hot electrons, SC is the metal-semiconductor coupling probabil-

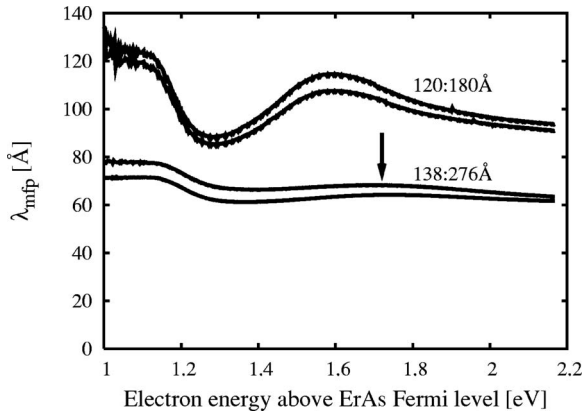

FIG. 3. Hot-electron mean free path in ErAs versus electron energy. The 120:180 Å traces are representative of the comparison between ErAs films 120 and 180 Å thick; the 138:276 Å traces result from comparisons between films of 138 and 276 Å. Two traces from each comparison are shown to illustrate the typical variation across different devices. The arrow points to the local maximum of the 138:276 Å traces.

ity, d is the base thickness, and P is the energy distribution of tunnel current.

Since tunneling is strongly energy dependent, electrons near the Fermi energy in the emitter are more likely to tunnel through the oxide barrier. P is therefore a function strongly peaked near $E=eV_{EB}$.[19] We replace this unknown function with the delta function: $P(E,V_{EB})\rightarrow I_t(V_{EB})\delta(E-eV_{EB})$, where $I_t(V_{EB})$ is the emitter tunnel current. This allows us to easily evaluate the integral in Eq. (1) and then divide both sides by $I_t(V_{EB})$ to yield

$$R(V_{EB}) = e^{-d/\lambda(V_{EB})}SC(V_{EB}), \tag{2}$$

where $R(V_{EB})=I_c(V_{EB})/I_t(V_{EB})$. This equation could be solved for λ if we could determine the function $SC(V_{EB})$. However, $SC(V_{EB})$ is a property of the ErAs/GaAs interface and is independent of the ErAs film thickness. We can therefore collect data on two transistors with different base thicknesses and solve Eq. (2) for each transistor. By dividing these two equations, we can solve for λ:

$$\lambda = \frac{d_2 - d_1}{\ln R_1 - \ln R_2}, \tag{3}$$

where R_1 and R_2 are the results of solving Eq. (2) for two transistors with base thicknesses d_1 and d_2, respectively. In Fig. 3 we see the result of this analysis applied to the corrected data of Fig. 2. Here we have used $d=d_{\mathrm{Al}}+d_{\mathrm{ErAs}}$ and assumed d_{Al} to be constant across samples grown during the same growth run. The comparison between $d_{\mathrm{ErAs}}=120$ and 180 Å yields $\lambda\sim 100$ Å, while the comparison between samples with $d_{\mathrm{ErAs}}=138$ and 276 Å gives $\lambda\sim 75$ Å. The variation in mean free path between sample sets could be due to a thickness-dependent mean free path, multiple electron reflections within the base layer, or differences in Al layer thickness between samples. A thickness-dependent mean free path is plausible because of the strain from the slight lattice mismatch between ErAs and GaAs [~1.6% (Ref. 1)]. As thicker layers are grown andthe lattice relaxes to its equilibrium value, this could introduce scattering which would lower the mean free path. Multiple reflections within the base layer have been observed in other systems,[20] and lead to a mean free path that appears thickness dependent.

The features in the data of Fig. 3, such as the local maximum in λ near 1.6 eV in the 120:180 Å trace and, indicated by the arrow, near 1.7 eV in the 138:276 Å trace, are presumably due to band structure effects in the ErAs. An investigation of the calculated ErAs band structure[21] shows a pair of large spikes in the density of states near 1.5 eV, with a relatively small density of states in the surrounding energies. These states appear to be located away from Γ but are otherwise distributed throughout the Brillouin zone. In the case of InGaAs, Seo *et al.* observed a sharp decrease in the transfer ratio of hot electrons once their energy was sufficient to reach the L valley of the conduction band.[22] It is conceivable that we are observing a similar phenomenon in ErAs, and that carriers in the states with high effective mass have an increased transit time through the ErAs layer and therefore experience a decreased mean free path. The two energy regions of lower mean free path in Fig. 3 would then correspond to the two spikes in density of states, with a region of longer mean free path between them. However, the features in Fig. 3 occur at slightly higher energies and are wider than the band structure calculation[21] predicts. This should be expected in light of the aforementioned base-contact resistance problem and the coarse resolution of the calculation. We will discuss the likelihood that this scenario is responsible for the features of Fig. 3 after first demonstrating that the features are not simply artifacts of our analysis.

One might speculate that these features are due to improper assumptions in our analysis. The actual emitter current distribution is not as strongly peaked as a delta function and has a nonzero width; could this result in fluctuations such as those seen in Fig. 3? We address this concern by treating the emitter energy distribution as a pair of weighted delta functions rather than a single delta function and observing the effect on the mean free path:

$$P(E,V) \rightarrow I_t(V)[\alpha\delta(E-eV) + \beta\delta(E-eV+\Delta)], \tag{4}$$

where $\alpha+\beta=1$. In this case some electrons come from an energy Δ below the Fermi energy in the emitter. Following the derivation above, we have

$$\frac{R_1(V)}{R_2(V)} = \frac{\alpha e^{-d_1/\lambda(eV)}SC(V) + \beta e^{-d_1/\lambda(eV-\Delta)}SC(eV-\Delta)}{\alpha e^{-d_2/\lambda(eV)}SC(V) + \beta e^{-d_2/\lambda(eV-\Delta)}SC(eV-\Delta)}. \tag{5}$$

Assuming that the variation in the metal-semiconductor coupling probability SC is negligible over the (short) interval $eV-\Delta\rightarrow eV$, we can reduce Eq. (5) to

$$\frac{R_1(V)}{R_2(V)} = e^{(d_2-d_1)/\lambda_a}\left[\frac{1+\frac{\beta}{\alpha}e^{d_1/\lambda_a - d_1/\lambda_b}}{1+\frac{\beta}{\alpha}e^{d_2/\lambda_a - d_2/\lambda_b}}\right], \tag{6}$$

where $\lambda_a=\lambda(eV)$ and $\lambda_b=\lambda(eV-\Delta)$. If we take the natural log of both sides and use the relation

$$1/\lambda_a - 1/\lambda_b = \frac{\lambda_b - \lambda_a}{\lambda_a \lambda_b} = \frac{\Delta}{\lambda_a \lambda_b}\frac{\lambda_b - \lambda_a}{\Delta} = -\frac{\Delta\lambda'}{\lambda_a \lambda_b} \tag{7}$$

and approximations to first order in Δ and β, respectively,

$$1 + \frac{\beta}{\alpha} e^{-\Delta\lambda' d/(\lambda_a \lambda_b)} \approx 1 + \frac{\beta}{\alpha}\left(1 - \frac{\Delta\lambda'}{\lambda_a \lambda_b} d\right), \tag{8}$$

$$\ln\left[1 + \frac{\beta}{\alpha}\left(1 - \frac{\Delta\lambda'}{\lambda_a \lambda_b} d\right)\right] \approx \frac{\beta}{\alpha}\left(1 - \frac{\Delta\lambda'}{\lambda_a \lambda_b} d\right), \tag{9}$$

then we arrive at

$$\ln\left(\frac{R_1}{R_2}\right) = (d_2 - d_1)\left(\frac{1}{\lambda_a} + \frac{\beta}{\alpha}\frac{\Delta\lambda'}{\lambda_a \lambda_b}\right). \tag{10}$$

By solving for the right hand side of Eq. (3), we can see the effect of broadening on our estimate of the mean free path

$$\frac{d_2 - d_1}{\ln R_1 - \ln R_2} = \frac{\lambda_a}{1 + \frac{\beta}{\alpha}\frac{\Delta\lambda'}{\lambda_b}}. \tag{11}$$

Let us consider the instance in which λ increases with increasing energy ($\lambda' > 0$). According to Eq. (11), the actual mean free path λ_a is decreased by a factor of $1/(1+\eta)$, where η is a small number. This underestimates the actual value by an amount that is larger for a more rapidly varying λ. The opposite is true in the case of $\lambda' < 0$; a quickly decreasing λ will be overestimated. The net effect is an estimate of λ that behaves as a smoothed version of the true mean free path. This is not unexpected since in essence our experiment convolutes the electron energy distribution with $\lambda(E)$, and convolution can be thought of as a smoothing operation.[23] Therefore we see that the mean free path indicated by our delta function analysis in Fig. 3 does reflect the true nature of the energy dependence, and the real variation may actually be more pronounced than our analysis indicates.

Since the features of Fig. 3 are not simply an artifact of our delta-function analysis, they must have a physical origin. In the ideal case, the only variation between devices is the ErAs film thickness, and in that case, the only possibility is that the features of Fig. 3 represent the actual energy dependence of the mean free path in ErAs. The rapid fluctuations would then likely be the result of variations in band structure and effective mass. However, this explanation does not account for the difference in relative size of the features between the 120:180 Å and 138:276 Å traces. If it were purely a band structure effect, one might expect the features to be preserved or even enhanced for thicker films, but in our case the 138:276 Å traces exhibit smaller fluctuations than the 120:180 Å traces.

Because our analysis isolates the ErAs mean free path by comparing multiple devices, any unintentional difference between the devices can lead to an inaccurate determination of the mean free path. This raises the question of how sensitive our measurement is to unintentional differences between devices and whether those differences could lead to features in the mean free path such as those observed in Fig. 3.

In these devices, electrons pass through a series of interfaces, and transport across any one of them could depend nonmonotonically on electron energy. However, two of them (the ErAs/GaAs and the Al/ErAs) are formed in a very controlled manner and thus should be identical in all devices. The other two interfaces (the Al/Al_2O_3 and the Al_2O_3/Al) are not as well controlled, but these comprise the emitter tunnel junction, which can be independently monitored via the emitter current (not shown). The current-voltage profiles of the emitter structures do not exhibit any fine structure that would indicate conductance channels, and the magnitude varies at most by a factor of 3 across all samples used in the analysis. More importantly, this variation is random across different devices, and therefore we can conclude that the features present in Fig. 3 are not likely to be the result of differences in emitter structures between samples.

Another possible source of error is the base-contact resistance, which, as mentioned above, can lead to errors in the determination of the energy of the tunneling electrons. However, as in the case of the tunnel junctions, the variation of the base-contact resistance is random across devices and is too small to account for the variations seen in Fig. 3.

Another parameter that is difficult to control between samples is the Al layer thickness within the base. As was mentioned previously, the Al layer thickness was not actively monitored during deposition and could only be estimated based on the Al flux rate. This resulted in variations between sets of samples, as evidenced by the negative mean free path we obtained when comparing the 120 Å sample with the 138 Å sample (not shown). Since Al also exhibits a mean free path of $\sim$100 Å,[24] evidently the Al layer on the 120:180 Å set of samples is more than 18 Å thicker than that of the 138:276 Å set. This is what prevents us from making cross comparisons between the sample sets (e.g., 120:276 Å and 138:180 Å).

We assume that the thickness variation between samples of the same set is negligible since they were done in the same growth run with the same Al flux rate, but we have no verification that this is the case. If there were variations in Al layer thicknessbetween samples of the same set, it could account for the overall difference in the mean free path between sample sets. For example, if the 120 Å sample had an anomalously thick Al layer, then comparisons from the 120:180 Å sample set would overestimate the mean free path.

However, a variation in Al layer thickness would not explain the fluctuations unless there were features within the Al mean free path. Since there is likely to be only a small Al layer thickness difference between samples from the same growth run, the Al mean free path variations would have to be very pronounced to produce the features seen in Fig. 3. Although we think this is unlikely, we could not find experimental evidence in the literature with sufficient energy resolution to rule out this possibility. In either event, the feature seems likely to be due to a true variation in the mean free path, whether it is due to ErAs or Al or some combination of the two.

In conclusion, we have used an ErAs/metal-base hot-

electron transistor structure to investigate the hot-electron mean free path in ErAs thin films grown on GaAs(100) at 80 K. By comparing films of thickness 120 and 180 Å, we find $\lambda \sim 100$ Å. For films with a larger difference in thickness, 138 and 276 Å, we find $\lambda \sim 75$ Å. Considering various sources of error in our measurement, we determine $\lambda \sim 100$ Å to be a reasonable estimate. Knowledge of this parameter should be useful when designing ErAs-based devices with a significant electron population ~1 eV above the ErAs Fermi level, such as thermionic energy conversion devices and Schottky barrier photodetectors.

This work was supported by the Office of Naval Research through ONR/MURI and by NSF/NNIN through the use of their facilities at Harvard University's Center for Nanoscale Systems (CNS).

*Electronic address: krussell@deas.harvard.edu

[1] C. J. Palmstrom, N. Tabatabaie, and S. J. Allen, Appl. Phys. Lett. **53**, 2608 (1988).
[2] Dmitri O. Klenov, Joshua M. Zide, Jeramy D. Zimmerman, Arthur C. Gossard, and Susanne Stemmer, Appl. Phys. Lett. **86**, 241901 (2005).
[3] Dmitri O. Klenov, Daniel C. Driscoll, Arthur C. Gossard, and Susanne Stemmer, Appl. Phys. Lett. **86**, 111912 (2005).
[4] Jeramy D. Zimmerman, Elliott R. Brown, and Arthur C. Gossard, J. Vac. Sci. Technol. B **23**, 1929 (2005).
[5] A. C. Young, J. D. Zimmerman, E. R. Brown, and A. C. Gossard, Appl. Phys. Lett. **87**, 163506 (2005).
[6] A. C. Young, J. D. Zimmerman, E. R. Brown, and A. C. Gossard, Appl. Phys. Lett. **88**, 073518 (2006).
[7] R. P. Prasankumar, A. Scopatz, D. J. Hilton, A. J. Taylor, R. D. Averitt, J. M. Zide, and A. C. Gossard, Appl. Phys. Lett. **86**, 201107 (2005).
[8] J. E. Bjarnason, T. L. J. Chan, A. W. M. Lee, E. R. Brown, D. C. Driscoll, M. Hanson, A. C. Gossard, and R. E. Muller, Appl. Phys. Lett. **85**, 3983 (2005).
[9] Jon E. Bjarnason and Elliott R. Brown, Appl. Phys. Lett. **87**, 134105 (2005).
[10] D. C. Driscoll, M. P. Hanson, A. C. Gossard, and E. R. Brown, Appl. Phys. Lett. **86**, 051908 (2005).
[11] J. M. Zide, D. O. Klenov, S. Stemmer, A. C. Gossard, G. Zeng, J. E. Bowers, D. Vashaee, and A. Shakouri, Appl. Phys. Lett. **87**, 112102 (2005).
[12] Gehong Zeng, John E. Bowers, Joshua M. O. Zide, Arthur C. Gossard, Woochul Kim, Susanne Singer, Arun Majumdar, Rajeev Singh, Zhixi Bian, Yan Zhang, and Ali Shakouri, Appl. Phys. Lett. **88**, 113502 (2006).
[13] J. M. O. Zide, A. Kleiman-Shwarsctein, N. C. Strandwitz, J. D. Zimmerman, T. Steenblock-Smith, and A. C. Gossard, Appl. Phys. Lett. **88**, 162103 (2006).
[14] K. J. Russell, I. Appelbaum, V. Narayanamurti, M. P. Hanson, and A. C. Gossard, Phys. Rev. B **71**, 121311(R) (2005).
[15] W. J. Kaiser and L. D. Bell, Phys. Rev. Lett. **60**, 1406 (1988).
[16] L. D. Bell and W. J. Kaiser, Phys. Rev. Lett. **61**, 2368 (1988).
[17] V. Narayanamurti and M. Kozhevnikov, Phys. Rep. **349**, 447 (2001).
[18] J. Smoliner, D. Rakoczy, and M. Kast, Rep. Prog. Phys. **67**, 1863 (2004).
[19] Ian Appelbaum and V. Narayanamurti, Phys. Rev. B **71**, 045320 (2005).
[20] P. L. de Andres, F. J. Garcia-Vidal, K. Reuter, and F. Flores, Prog. Surf. Sci. **66**, 3 (2001).
[21] Takashi Komesu, Hae-Kyung Jeong, Jaewu Choi, C. N. Borca, P. A. Dowben, A. G. Petukhov, B. D. Schultz, and C. J. Palmstrom, Phys. Rev. B **67**, 035104 (2003).
[22] K. Seo, M. Heiblum, C. M. Knoedler, W-P. Hong, and P. Bhattacharya, Appl. Phys. Lett. **53**, 1946 (1988).
[23] Albert F. Carley and Richard W. Joyner, J. Electron Spectrosc. Relat. Phenom. **16**, 1 (1979).
[24] S. M. Sze, C. R. Crowell, G. P. Carey, and E. E. La Bate, J. Appl. Phys. **37**, 2690 (1966).